Understanding catalytic reactions over zeolites: A density functional theory study of selective catalytic reduction of NOX by NH3 over Cu-SAPO-34

Mao, Y., Wang, Z., Wang, H.-F., & Hu, P. (2016). Understanding catalytic reactions over zeolites: A density functional theory study of selective catalytic reduction of NOX by NH3 over Cu-SAPO-34. *ACS Catalysis*. Advance online publication. https://doi.org/10.1021/acscatal.6b01449

Published in:
ACS Catalysis

Document Version:
Peer reviewed version

Article

Understanding catalytic reactions over zeolites: A density functional theory study of selective catalytic reduction of NOX by NH3 over Cu-SAPO-34

Yu Mao, Ziyun Wang, Hai-Feng Wang, and Peijun Hu

ACS Catal., **Just Accepted Manuscript** • DOI: 10.1021/acscatal.6b01449 • Publication Date (Web): 11 Oct 2016

Understanding catalytic reactions over zeolites: A density functional theory study of selective catalytic reduction of NO_x by NH_3 over Cu-SAPO-34

Yu Mao,[†,‡] Ziyun Wang,[‡] Hai-Feng Wang,[*,†] and P. Hu[*,†,‡]

†*Key Laboratory for Advanced Materials, Centre for Computational Chemistry and Research Institute of Industrial Catalysis, East China University of Science and Technology, 130 Meilong Road, Shanghai, 200237, China.*

‡*School of Chemistry and Chemical Engineering, The Queen's University of Belfast, Belfast, BT9 5AG, United Kingdom.*

E-mail: hfwang@ecust.edu.cn; p.hu@qub.ac.uk

Abstract

Metal exchanged CHA-type (SAPO-34 and SSZ-13) zeolites are promising catalysts for selective catalytic reduction (SCR) of NO_x by NH_3. However, the understanding of the process at the molecular level is still limited, which hinders the identification of its mechanism and the design of more efficient zeolite catalysts. In this work, modelling the reaction over Cu-SAPO-34, a periodic density functional theory (DFT) study of NH_3-SCR was performed using hybrid functional with the consideration of van der Waals (vdW) interactions. A mechanism with a low N–N coupling barrier is proposed to account for the activation of NO. The redox cycle of Cu^{2+} and Cu^{+}, which is crucial for the SCR process, is identified with detailed analyses. Besides, the decomposition of NH_2NO is shown to readily occur on the Brønsted acid site by a hydrogen push-pull mechanism, confirming the collective efforts of Brønsted acid and Lewis acid (Cu^{2+}) sites. The special electronic and structural properties of Cu-SAPO-34 are demonstrated to play an essential role the reaction, which may have a general implication on the understanding of zeolite catalysis.

Keywords

Density functional theory, Selective catalytic reduction, Cu-SAPO-34, Ammonia, Zeolite, Nitric oxide

Introduction

The reduction of environmentally harmful nitrogen oxides (NO_x), especially for these in lean-burn engine exhausts, is currently an important and challenging task for chemical researchers.[1–4] Among possible solutions, selective catalytic reduction (SCR) of NO_x by ammonia (NH_3-SCR) over metal-exchanged CHA-type zeolites has attracted great attention in recent years. As the major N-containing compounds from diesel engines is NO (>90%), the

main reaction of NH_3-SCR can be expressed as:[5]

$$4NH_3 + 4NO + O_2 \longrightarrow 4N_2 + 6H_2O \quad (1)$$

which is usually called the standard SCR. The process with equimolar mixture of NO and NO_2, on the other hand, is named the fast SCR that reacts much faster:[6]

$$2NH_3 + NO + NO_2 \longrightarrow 2N_2 + 2H_2O \quad (2)$$

Prior to zeolites, NH_3-SCR techniques have been used with noble metals and metal oxides (*e.g.*, V_2O_5-based catalysts) in stationary plants.[7–9] However, due to the toxicity of V_2O_5 species and different catalytic conditions of automobile engines,[10] zeolites have received great attention as potential NH_3-SCR catalysts nowadays. Among all zeolites, a majority of studies in past decade were conducted on copper exchanged small-pore CHA-type zeolites (Cu-SAPO-34 and Cu-SSZ-13) because of their high NO_x conversion as well as high N_2 selectivity, non-toxicity, wider operation temperature ranges, and excellent hydrothermal stability in diesel engines.[2–4,10–12] Cu-SSZ-13 is now in commercial use[13] and received much attention in past several years; SAPO-34 has the same topology with SSZ-13, but with different silica ratio. Kwak *et al.*[14] demonstrated that Cu-SSZ-13, compared with Cu-beta and Cu-ZSM-5, was more active in SCR over the entire temperature range and more selective towards nitrogen formation (less NO_2 and N_2O by-products). Ma *et al.*[15] reported that Cu-SAPO-34 would be more active than Cu-SSZ-13 after hydrothermal treating.

There are two kinds of possible active sites in Cu exchanged CHA-type zeolites: the Brønsted acid (H in the zeolite framework) and Lewis acid (introduced Cu ion) sites. For the Cu sites, diffuse reflectance infrared fourier transform (DRIFT) spectroscopy and X-ray absorption spectroscopy (XAFS) showed that they would locate in both six- and eight-membered ring.[12,16–18] Catalytic experiments of Beale *et al.*[19] revealed that the mononuclear Cu^{2+} in six-membered rings is responsible for N_2 production, while the Cu in eight-membered

ring ($CuAlO_2$) appears to promote the formation of undesired N_2O. They pointed out that the SCR activity is inexorably linked with isolated Cu on the six-membered ring. DFT calculations also indicated that isolated Cu ions prefer to lie slightly above the six-membered ring of CHA-type zeolites.[20–28 25,29–32] When Cu loading is high, Cu dimers would be formed in the zeolites,[33] yet they may not be directly related with SCR reactivity.[11] Xue *et al.*[34] reported that the TOF value of SCR would be a function of isolated Cu^{2+} amount over Cu-SAPO-34. For Brønsted acids, it is currently not well understood what role it is in reaction system. Some studies showed that the Brønsted acid site could catalyse part of the reaction,[6,35,36] while others argued that its effect is rather limited.[11,25,37]

The nature of Cu species during the reaction is more complicated. According to the latest research of Schneider *et al.*[12] the oxidation state and coordination environment of Cu would vary as a function of environmental conditions. For example, upon adsorption of NH_3, NO, or H_2O on the Cu atoms in six-membered ring, the Cu atoms may be lift out from their original position into the larger cavities to form Cu complexes,[38–40] such as $Cu(H_2O)_6$ and $Cu(NH_3)_6$.[16,25,33,41,42] But only Cu sites near six-membered rings seem to contribute to SCR activity in CHA-type zeolites.[19,24,25,43] Furthermore, many studies[11,23,28,44,45] suggested that a mixture of Cu(I)–Cu(II) oxidation states co-exist during the standard SCR, and the SCR process will be accompanied by a redox cycle of Cu^+ and Cu^{2+}. Initially, Cu^{2+} in the zeolites would be reduced to Cu^+ by the adsorption of NO and NH_3 to form N_2 and H_2O.[28,46,47] NO oxidation then takes place on the Cu^+ site, regenerating Cu^{2+} that completes the redox cycle.[11,28] The presence of Cu^+ was identified by many experimental investigations, including X-ray photoelectron spectroscopy (XPS) and infrared spectroscopy (IR).[23,25,34,44,48]

Furthermore, the reaction rate of fast SCR (equation 2) is much higher than the standard SCR (equation 1), the intrinsic reason of which is still under debate. Most studies suggested that in the standard SCR process, NO oxidation to NO_2 by O_2 is the rate-limiting step,[11] and thus it is much slower than fast SCR which did not require O_2 to oxidise NO. For example, Janssens *et al.*[11] proposed that NO and O_2 would react on the Cu^+ site to form

NO_3^-, which would further react with NO to produce NO_2^- and NO_2. In the fast SCR, NO and NO_2 could also bind in the gas phase to form N_2O_3, followed by a hydrolysis to nitrous acid ($N_2O_3 + H_2O \longrightarrow 2\,HONO$).[36,49] After that, NH_3 can easily react with HONO to form NH_4NO_2 that decomposes readily to yield N_2 and H_2O under reaction conditions.[2,10,15] Tronconi *et al.*,[50] however, challenged this explanation using the experimental observation that rate of NO oxidation over zeolites is much slower than the standard SCR.

In addition to above studies, numerous investigations have been carried out on NH_3-SCR over zeolites; however, several fundamental issues about its mechanism are still not well understood due to the limitations of current experimental techniques on detecting dynamic and instant events at the molecular level.[4] The large number of possible reactions in SCR system also makes reaction pathways very complicated. Some important questions remain to be answered: (i) how NO is activated and what the role of O_2 is; (ii) whether the redox cycle of Cu^{2+} and Cu^+ is involved and what the redox mechanism is; (iii) whether both Brønsted acid and Lewis acid collectively catalyse the SCR process. To elucidate these questions, several theoretical attempts have been made by Li *et al.*[6,36] and Bruggemann *et al.*[35,51] on H-form and Fe exchanged zeolites with cluster models, and some possible reaction pathways were identified. Paolucci *et al.*[28] proposed a detailed NH_3-SCR mechanism on Cu-SSZ-13 using both operando X-ray absorption experiments and density functional theory (DFT) calculations. $Cu^{I}H_2NNO/H^+$ and $Cu^{II}NO_2/NH_4^+$ complexes, according to their study, were involved in the reducing and oxidising parts of the whole reaction, respectively. Very recently, Janssens *et al.*[11] proposed a consistent scheme of NH_3-SCR over Cu-SSZ-13. They described a complete catalytic cycle with correct stoichiometry while allowing adsorption and desorption of stable molecules only. Despite aforementioned studies, a comprehensive first principles investigation of NH_3-SCR over Cu-SAPO-34, to the best of our knowledge, has not been performed yet. In this contribution, we explore the reaction by DFT calculations with hybrid (HSE06) functional to answer above three questions. Van der Waals (vdW) interactions were also included to accurately describe the system. A detailed step-by-step NH_3-SCR

mechanism over Cu-SAPO-34 were obtained with moderate energy barriers and reasonable intermediate structures. Our results show that the high activity of zeolites on catalysing NH_3-SCR are closely related to their structural and electronic properties, including special six-membered ring structure, influence of the framework H on the valence of loaded metal ion, and collective efforts by Brønsted acid and Lewis acid sites. Our study extends beyond what have been published on SSZ-13, providing both insight into SCR catalysts and zeolite chemistry.

Computational methods

All calculations in the paper were carried out with the Heyd–Scuseria–Ernzerhof (HSE06) functional[52–54] using the Vienna ab initio simulation package (VASP).[55,56] The D3 correction method[57] was employed in order to include van der Waals (vdW) interactions, which may not be ignorable in zeolites due to their porous structure. The project-augmented wave (PAW) method was used to represent the core–valence interaction.[58,59] For the calculations of total energy, a cut-off energy of 400 eV was set for plane wave basis sets to expand the valence electronic states and spin-polarization was included. Transition states (TS) were determined by a constrained optimization scheme,[60,61] in which TSs are verified until (i) all forces on atoms vanish and (ii) the total energy reaches maximum along the reaction coordination but minimum with respect to the rest of the degrees of freedom. For computational efficiency, the geometrical optimization was firstly calculated by Perdew–Burke–Ernzerhof (PBE) functional;[62] all atoms were fully relaxed until the forces were lower than 0.05 eV/Å. Then HSE06 functional was employed to obtain the accurate total energy. To obtain the free energy of species, some standard formulas of statistical mechanics were used to calculate the thermodynamic correction including zero-point-energy (ZPE), thermal energy and entropy derived from partition functions.[63,64] (see SI-1 for details).

As we mentioned in the introduction, SAPO-34 is a specific type of silicoaluminophos-

phate zeolite with chabazite (CHA) structure;[65] the composition of unit cell is $H_xSi_xAl_6P_{6-x}O_{24}$. Experimentally, the of Si in SAPO-34 (Si/(Si+Al+P)) is usually larger than 0.1,[66,67] and the value of x can be up to 1.32 as a result of magic-angle spinning NMR analysis.[68,69] In this work, we built a Cu-SAPO-34 ($1 \times 1 \times 2$) supercell with a x value of 1.5 to represent the zeolite. Two H atoms were removed from the supercell to compensate the positive charge of the introduced Cu^{2+} ion, and the final chemical formula of the supercell is $CuHSi_3Al_{12}P_9O_{48}$. Similar models have been employed by Termath *et al.*[70] and Uzunova *et al.*[68,71,72] This model is reasonable for investigating the NH_3-SCR process since both Brønsted acid (H) and Lewis acid (Cu) are included in the supercell. During the calculations, the Brillouin zone was sampled at the gamma point, which is appropriate for this insulator.[12] The adsorption energy (ΔG_{ad}) was defined as:

$$\Delta G_{ad} = G_{adsorbate+zeolite} - G_{adsorbate} - G_{zeolite} \quad (3)$$

where $G_{zeolite}$, $G_{adsorbate}$, and $G_{adsorbate+zeolite}$ are the free energies of the zeolite, adsorbate in the gas phase, and adsorbate adsorbed on the zeolite, respectively.

Results and discussion

Structure of the Cu-SAPO-34 and the adsorption of gas phase molecules

The optimized Cu-SAPO-34 supercell is displayed in Fig. 1. Under low Cu loading content, as mentioned in the introduction, Cu was suggested to locate slightly above the six-membered ring near two Si atoms (position 1 in Fig. 1b)[2,14] as a divalent ion (Cu^{2+}). To validate this view, we examined the energies of Cu-SAPO-34 with Cu^{2+} in different positions (1–5 in Fig. 1b) and ensured that position 1 is the most stable one (Tab. S1 in SI). We can see from the figure that Cu is coordinated with four O atoms in the six-membered ring with distances of 2.08, 1.95, 1.91, and 2.36 Å, which are quite similar to the results of Uzunova *et al.*[68,71,72]

There are two Si atoms in the ring, while the remaining Si is accompanied by a H atom to form a Brønsted acid site. The stabilities of different H positions (1–4 in Fig. 1a) were also tested. Positions 1–4 show very close stabilities, among which position 1 is slightly preferable (Tab. S2 in SI). The volume of the relaxed supercell was calculated to be 1662.5 $Å^3$, very close to the experimental value (1644.8 $Å^3$).[69,73]

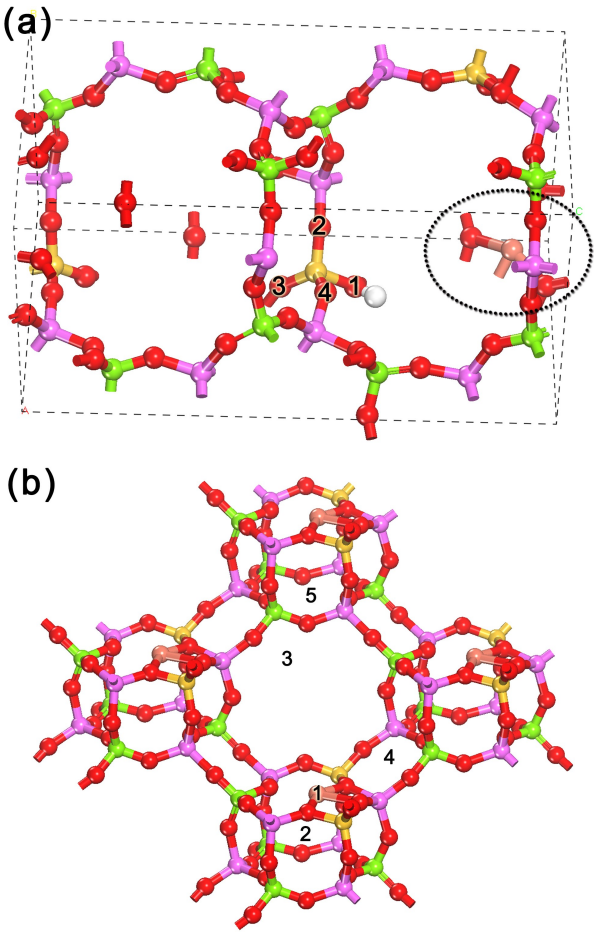

Figure 1: Structural illustrations of the (a) Cu-SAPO-34 supercell; (b) periodic view of the elliptical circle in (a). Green, red, purple, yellow, brown, and white balls represent P, O, Al, Si, Cu, and H atoms, respectively. This notation will be used throughout the paper.

In reaction equations (1) and (2), the reactants of SCR are NH_3, NO, O_2, and NO_2. We subsequently investigated the adsorption of these species and water on both Brønsted acid (B-site) and Lewis acid (L-site) sites, the best adsorption structures of which are illustrated in Fig. 2. In the figure, H_2O exhibit moderate adsorption on B- and L-sites, while both NO_2

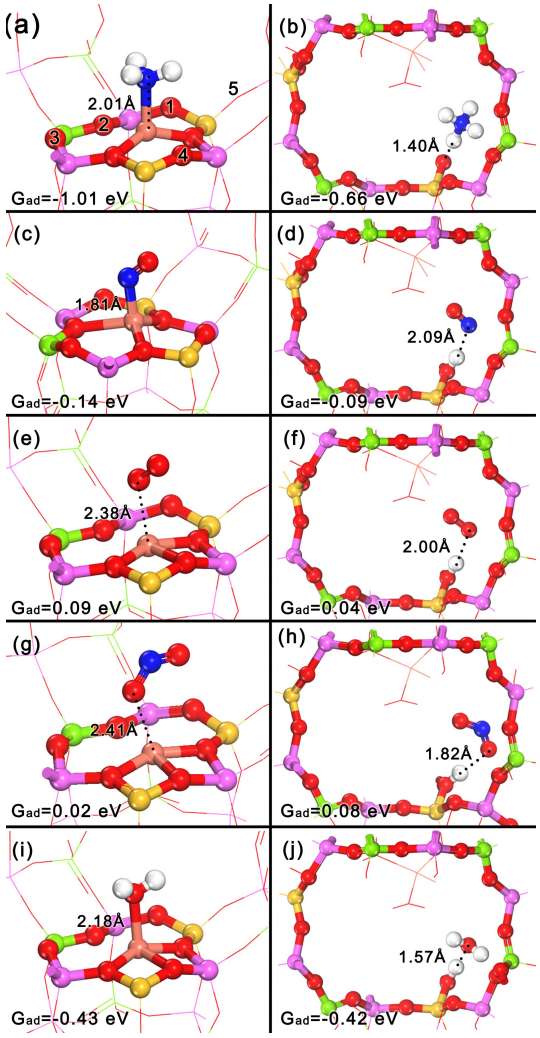

Figure 2: Structural illustration of the adsorption of NH_3 (ab), NO (cd), O_2 (ef), NO_2 (gh), and H_2O (ij). The left and right columns refer to the Lewis acid (Cu^{2+}) and Brønsted acid (H) site, respectively.

and O_2 hardly adsorb on the zeolite. NO prefers to slightly bond with the Cu^{2+} ion by its N end. NH_3 binds strongly on both sites, and it will exist as NH_4^+ on B-sites. The results indicate that L-sites will be dominantly covered by NH_3 and a small amount of NO at the start of SCR process, and the B-site by NH_3. It is in accordance with the generally accepted opinion that NH_3 and NO shall react on L-sites whereas B-sites sever as a NH_3 reservoir in the beginning of the reaction.[4,74] The NH_3 on B-sites could migrate to L-sites as the reaction proceeds.

Formation of the N–N bond

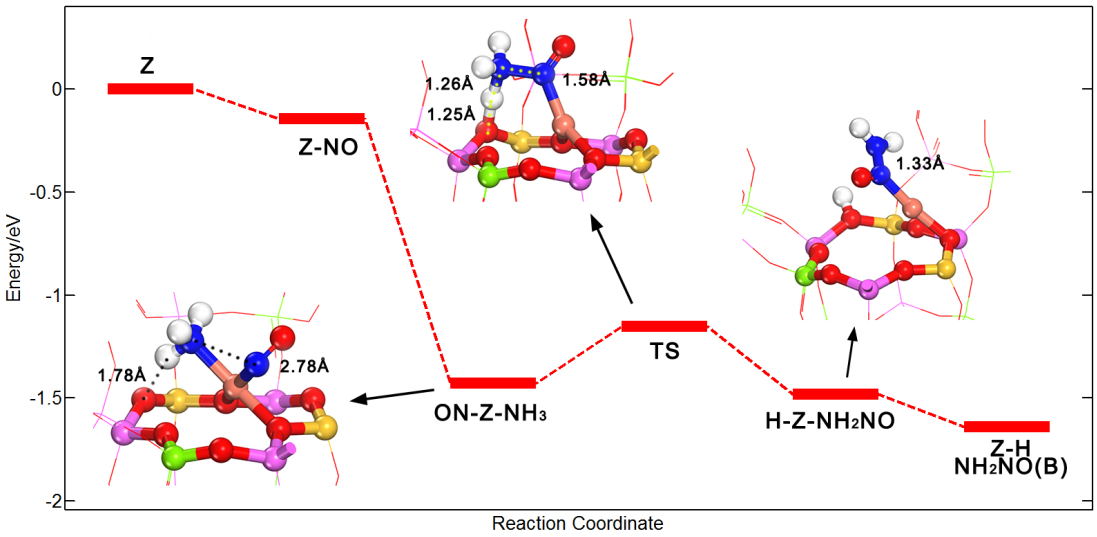

Figure 3: Free energy profile of the N–N coupling process. Some key structures are illustrated as inserts. (B) in the NH_2NO (B) indicates that it has been transferred to a Brønsted acid site.

The full mechanism of NH_3-SCR is considerably complicated.[3,10] Among that, N–N coupling is a crucial step towards the formation of nitrogen; therefore, it will be investigated first in this paper. Considering the valence of N in N_2 (0), the coupling of two N atoms shall come from NH_3 (-3) and NO (+2), respectively. According to this principle, we tried numerous possible reaction schemes of NO with NH_3 in order to form N–N bond, but all of them failed: a huge repulsion would occur when N in NO approaches NH_3; the NO would be pushed away if they are forced to be close. This is reasonable since N in NH_3 is saturated (Fig. 2a); therefore, the possibility of direct attacking of NO to NH_3 is ruled out. Then, in order to circumvent the problem of saturated NH_3, we tried to remove one H from the NH_3 to form NH_2 because NH_2 is unsaturated, which would be easier for NO to react. Five positions indicated in Fig. 2a were considered to locate H after NH_3 decomposition. However, from the results in Fig. S1, we found that all these pathways are extremely unfavourable thermodynamically; their free energies are 0.94 $\sim$ 1.98 eV higher than that in Fig. 2a, let alone kinetic barriers. So, it would be very difficult to directly remove one H from NH_3.

Since both of above reaction schemes are very difficult to occur over zeolites, we considered if other species in SCR reaction could facilitate the process. After numerous attempts and calculations, we found that with the assistance of NO, the N–H bond breaking would be much easier:

$$NH_3 + NO + Z \longrightarrow NH_2NO + Z{-}H \quad (4)$$

where Z indicates the zeolite. We subsequently investigated relevant intermediates and transition states of the reaction, whose structures and energies are displayed in Fig. 3. It proves that with NO, the reaction barrier would be much lower compared with dehydrogenation of NH_3 alone. In Fig. 3, NO and NH_3 would adsorb on the Cu^{2+} with considerable free energy declines (1.43 eV). It is worth noting that in the insert (ON-Z-NH_3) of Fig. 3, one H in the NH_3 is quite close to a framework O (1.78 Å), indicating a hydrogen bond interaction between them. Then, in the transition state, NH_3 would approach the framework O, intending to bond it with the H. The distance between two N atoms, at the same time, is shortened (1.58 Å). Finally, since the bonding of two N would release a large amount of energy compensating the energy needed to break the N–H bond in NH_3, two N atoms couple to form NH_2NO while the H remains on the framework O (insert H-Z-NH_2NO in Fig. 3). The energy barrier for this process was calculated to be 0.28 eV, an exceptionally small value, indicating that reaction 4 is a very effective way to activate the NO in NH_3-SCR. We further made a frequency analysis to ensure its accuracy. The results showed that the transition state here exhibited one and only one imaginary frequency, which corresponds to N–N coupling and N–H breaking with a value of $450.5i$ cm^{-1}. The NH_2NO would transfer to B-sites for further decomposition, which will be demonstrated in the last subsection. In addition, we made a Bader analysis on Cu ion before (Z) and after (Z-H) N–N coupling reaction, finding that the valence of Cu ion changes from 1.12 to 0.69 which means that Cu^{2+} is partly reduced to Cu^{+}. The result is quite reasonable, since we can see from the left column of Fig. 2 and schemes in Fig. 3 that before N–N coupling, Cu^{2+} ion tend to coordinate with four atoms, while the coordination number of Cu^{+}, after the reaction, becomes two (scheme H-Z-NH_2NO in Fig.

3). The results agree well with the general principle in coordination chemistry. Deep insight into the valence change of Cu ion and the intrinsic reason why the reaction can happen over zeolites by such an low-energy-barrier mechanism will be presented in the discussion section.

NO and Cu^+ oxidation by O_2

Although the whole reaction is the reduction of NO_x, O_2 plays a crucial role in the SCR process.[4,10] Some researchers argued that in standard SCR O_2 will oxidise NO into NO_2, resulting a fast SCR; however, other studies argued that standard and fast SCR may exhibit distinct mechanisms.[50,75] Currently, a clear mechanism for NO oxidation to NO_2 on the Cu ion is under debate and have not been achieved yet. Some previous studies stated that NO was oxidised by O_2 in the gas phase or in pores of zeolites ($O_2 + 2NO \longrightarrow 2\,NO_2$),[36] but it is a three-molecule reaction thus its contribution to the overall NO oxidation is limited. We suggest that the elementary reaction is

$$O_2 + NO + Z{-}H(Z{-}NH_4) \longrightarrow NO_2 + O* {-}Z{-}H(O* {-}Z{-}NH_4) \quad (5)$$

where the metal ion sites play the main role. Z-H in equation 5 means that a H resides on the framework O of the six-membered ring (Fig. S2a), and O* indicates an adsorbed O atom over the Cu ion. It should be noted that NH_3 can readily adsorb on this H site ($G_{ad} = -1.19$ eV), forming NH_4^+ on the ring (Z-NH_4, Fig. S2b). Then, we investigated the adsorption of O_2 on Cu ion site as well as the energy barriers and free energy change of above reaction, the energy diagrams of which are shown in Fig. 4.

From the results, we can notice that the adsorption energy of O_2 increases significantly after Cu^{2+} being reduced to Cu^+ with a H on the six-membered ring (G_{ad} from 0.52 eV to $\sim$ 0 eV). Then, effective energy barriers on Cu^+ site (Z-H 1.06 eV and Z-NH_4 0.86 eV) is found to be much lower than that on Cu^{2+} (3.65 eV). This agree well with the previous work that Cu^{2+} ions are incapable of activating O_2,[76] and Cu^+ plays role of catalysing NO

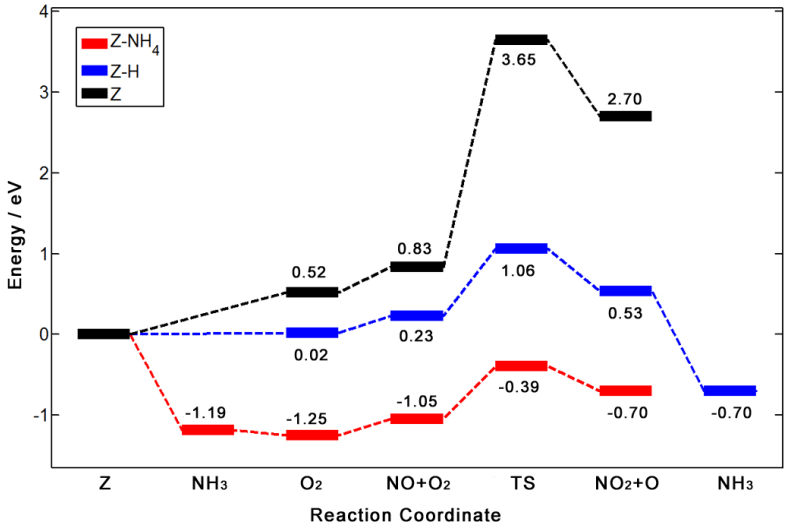

Figure 4: Free energy diagrams of O_2 oxidation on zeolite (Z, black), Z-H (blue), and Z-NH_4 (red). For Z and Z-H pathway, O_2 and NO will adsorb on Cu site and react to yield NO_2 and O through the transition state, NH_3 will adsorb on Z-H after that (corresponding to structures in Fig. S2(a, c) and Fig 5(b, d, f); for Z-NH_4 pathway, one NH_3 would adsorb first, then followed by O_2, NO adsorption and the transition state (corresponding to structures in Fig. S2(b, d) and Fig. S3(b, d, f))

oxidation.[11] We also considered the attacking of NO to O_2 from gas phase (Fig. S3(a, c, e) and Fig. 5(a, c, e)), the energy barriers of which are over 1 eV, unfavourable compared with NO and O_2 co-adsorbing on Cu site. After that, the produced NO_2 can react with its neighbouring NH_4^+ (Fig. S3f or Fig. 5f with NH_3 adsorption) to form NH_4NO_2, leaving an O atom over the zeolite. The left O atom is very active and can readily react with NO to form NO_2 with a considerable energy decline of 2.67 eV. Therefore, the NO oxidation reaction over Cu-SAPO-34 zeolites can be expressed as follows:

$$O_2 + 2\,NO + NH_3 + Z{-}H \longrightarrow NH_4NO_2 + NO_2 + Z \tag{6}$$

It is well recognized that NH_4NO_2 is easy to stoichiometrically decompose into N_2 and H_2O under SCR operation condition:[2,4,10,15]

$$NH_4NO_2 \longrightarrow N_2 + 2\,H_2O \tag{7}$$

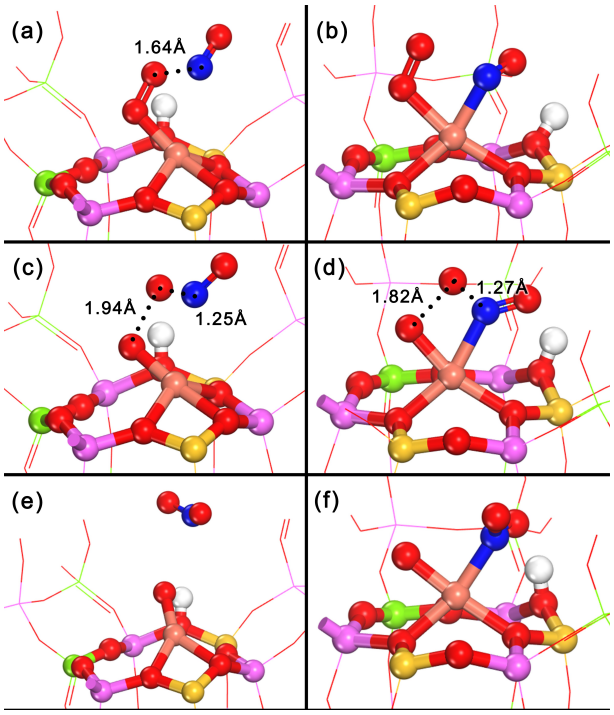

Figure 5: Structural illustration of NO oxidation on the reduced Cu ion site (Z-H). (a, b), (c, d), and (e, f) correspond to the initial, transition, and final states, respectively. In the left column, NO attacks from the gas phase while NO and O_2 co-adsorbed in the right.

To sum up, reaction 4 and 5 not only couple the N–N bond and form NH_2NO and NH_4NO_2, but also consist a redox cycle. Intuitively, the involvement of a redox cycle is quite reasonable because from equation 4 and 6, we can see that the reaction ratio of NH_3 and NO is 1:1, while the oxidation states of N in them is a mismatch (-3 in NH_3 and +2 in NO). Therefore, the coupling of N–N bond in NH_3 and NO must be accompanied by the reduction of L-site ($Cu^{2+} \longrightarrow Cu^{+}$) which will be regenerated by the oxidation of O_2. The redox cycle explains well the experimental observation that steady state NO conversion would decrease to zero after O_2 cut-off under standard SCR conditions.[28] According to their study, the content of Cu^{+} increases to 75–95% of the whole Cu species, and SCR reactions would be soon stopped since N–N coupling cannot happen on Cu^{+} site.

If we consider fast SCR (reaction 2) with NO_2 involved, NO oxidation is not necessary

after N–N coupling and the reaction goes as follows:

$$NO_2 + NH_3 + Z{-}H \longrightarrow NH_4NO_2 + Z \quad (8)$$

NO_2 and NH_3 can strongly adsorb on Cu^+ and framework H (G_{ad} = −0.86 and −1.19 eV in Fig. S2e and S2b, respectively), and NO_2 can naturally attack its neighbouring NH_4^+ to form NH_4NO_2 (Fig. S2f).[28]

After N–N coupling (equation 4) and NO oxidation (equation 6), the copper restores to Cu^{2+} and the remaining reactants for standard SCR are one NO, NO_2 and two NH_3. Interestingly, these are exactly the reactants of fast SCR (reaction 2), which would be complete through reaction 4, 8, and 7. It should be noted that we also tried another mechanism after NO oxidation, which is shown is supporting information 5.

NH_2NO decomposition into H_2O and N_2

The NH_2NO formed in above stages will decompose into H_2O and N_2 to complete the whole SCR process. Previous studies showed that it is a relatively easy process on the B-site of zeolites by a hydrogen push-pull mechanism.[35,36] We investigated its decomposition on both Brønsted acid and Lewis acid sites, and all intermediates and transition states were identified (Fig. S5). It can be seen from the scheme in Fig. 6 that the configuration of NH_2NO will change several times by the transferring of H atom, which was well recognised by previous studies.[36,77] We firstly tried this process on the L-site (Fig. S5), but the energy barrier of the first step of NH_2NO decomposition in L-acid, the proton transferring from N to O, was very high (2.03 eV). From Fig. S5b, we can see that during the intra-molecular proton transfer, an unstable four-membered ring is formed, exerting a strong steric hindrance and making L-side unfavourable for catalysing this reaction. On the other hand, energy barriers of the reactions on the B-site are moderate, making it easy to occur (the energy profile in Fig. 6, and corresponding structures in Fig. S6).

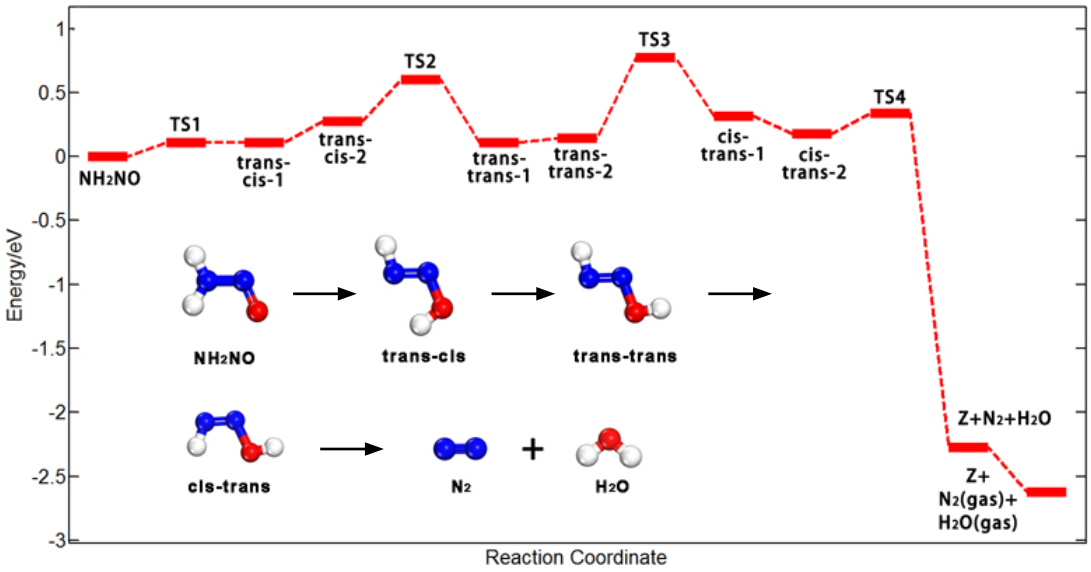

Figure 6: Total energy profile of NH_2NO decomposition on the B-site and a scheme of transformation of NH_2NO. Structures of intermediates and transition are displayed in Fig. S6.

As shown in Fig. S6a, NH_2NO adsorbs on the B-site by the interaction between O and H atoms, in which the B-site severs as a H reservoir, helping NH_2NO to transfer H by the so-called hydrogen push-pull mechanism. In the subsequent steps, NH_2NO transforms its configuration several times by donating and receiving H with the help of the framework and finally decomposes to N_2 and H_2O with considerable energy release. The highest effective barrier[63,78] for the NH_2NO decomposition is 0.77 eV (from NH_2NO to TS3), which is much lower than that on the L-site. The results show that Brønsted acid and Lewis acid (Cu^{2+}) sites would collectively catalyse NH_3-SCR over Cu-SAPO-34 zeolites.

Overall mechanism

An overall picture of NH_3-SCR over Cu-SAPO-34 is schematically illustrated in Fig. 7. To the best of our knowledge, it is the first time that such a step-by-step reaction pathways of NH_3-SCR over Cu-SAPO-34 is presented from periodic DFT calculations. For the standard SCR, the reaction is initialized by N–N coupling between NO and NH_3 that co-adsorbed on the Cu^{2+} site to form NH_2NO; then, NO is oxidised by O_2, which further react with

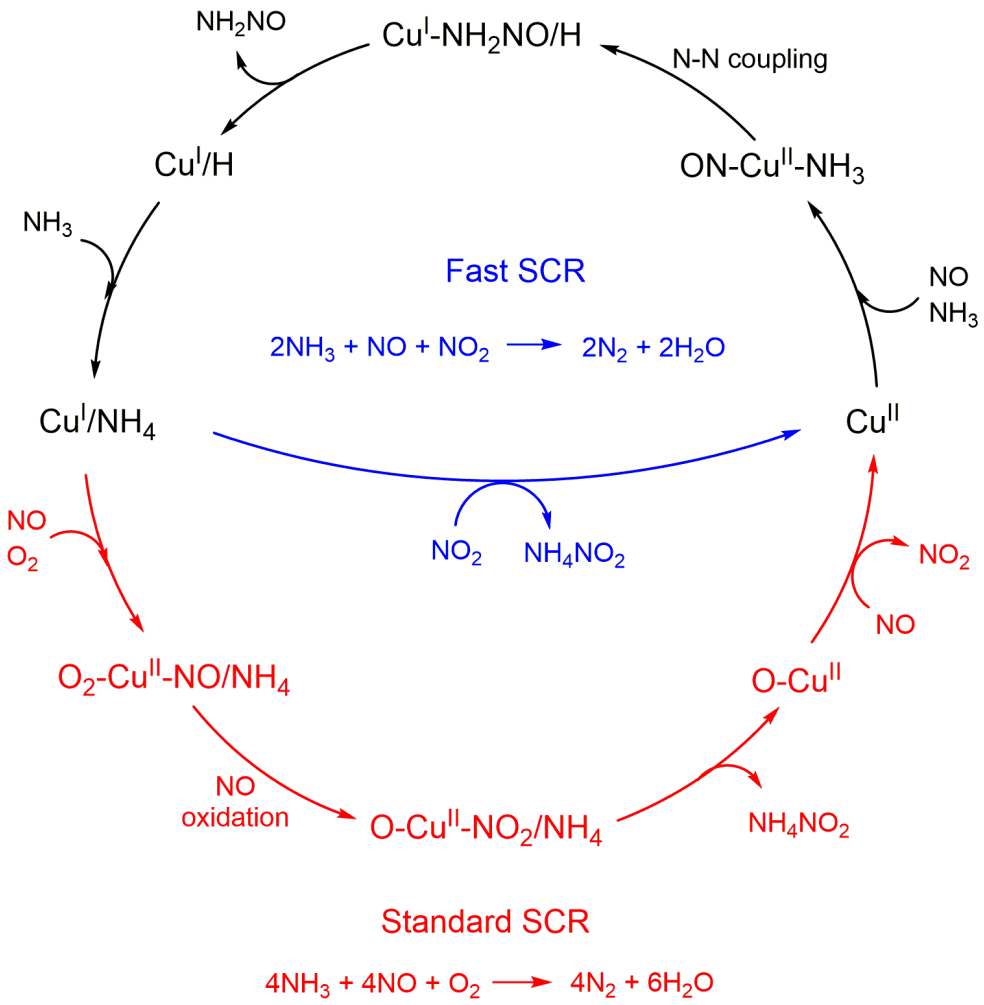

Figure 7: Schematic illustration of the mechanism of fast and standard NH_3-SCR over Cu-SAPO-34. It should be noted that NH_4NO_2 and NH_2NO will decompose to N_2 and H_2O stoichiometrically (equation 7 and scheme in Fig. 6), and it is not showed in the figure for clarity.

NH_3 to produce NH_4NO_2, leaving on O atom on the Cu site. After that, the O atom will further oxidise NO to yield NO_2. Next, the active site is restored to pure Cu^{2+} and react with remaining two NH_3, one NO and NO_2 to form one NH_4NO_2 and NH_2NO. Finally, NH_4NO_2 and NH_2NO decompose into N_2 and H_2O. Among all these process, the effective free energy barrier of NO oxidation is the highest (0.86 eV) and may thus be regarded as the rate-limiting step.

From the mechanism, we can notice that the standard SCR has to go through both NO activation (coupling with NH_3) and NO oxidation processes, which are closely related with

each other to ensure the whole reactions to be completed. Firstly, NO and NH_3 will couple with the assistance of O in the framework to produce NH_2NO and reduce Cu^{2+} to Cu^+. Then, NO will be oxidised over Cu^+ site to further form NH_4NO_2; however, in addition to producing NO_2, a more vital role of NO oxidation is to regenerate Cu^{2+} site to keep reactions on going. Without it, the zeolite will be soon saturated with reduced Cu^+ species, and the overall reaction will be stopped. With these two essential processes, the standard SCR can proceed continuously, producing N_2 by the stoichiometric decomposition of NH_4NO_2 and NH_2NO.

Comparing with Cu-SSZ-13, which is currently in commercial use and attracted most attentions in the past decades, our work represents one of few DFT studies on NH3-SCR mechanism over Cu-SAPO-34, well extending beyond what have been published on SSZ-13. The location of active Cu site, the redox cycle of Cu^+ and Cu^{2+}, and the coupling of N–N bond are quite similar on these two zeolites. Both NH_3 and NO are required for N–N coupling and Cu^{2+} would be reduced to Cu^+ to complete the reduction of the redox cycle, which is in agreement with experiments.[11,28] Some notable differences, on the other hand, appear on the NH_2NO decomposition and NO oxidation. Previous literatures suggested that the effect of Brønsted acid sites are rather limited.[11,25,37] It is found that the SCR activity under 473 K is not dependent on the amount of Brønsted acid sites. Based on this experimental observation, the Brønsted acid site may not be a part of SCR process, and thus it can only influence SCR activity by altering the acidity of zeolite or interacting with neighbouring Cu site. Gao *et al.*[17] pointed out that Brønsted acidity favors the standard NH_3-SCR without being an essential ingredient of the active site. However, according to our results, Brønsted acid sites are necessary for NH_2NO decomposition which is difficult to occur on Cu sites. Through a hydrogen push-pull mechanism, we showed that Brønsted acid sites could readily catalyse the decomposition of NH_2NO, also in agreement with some theoretical studies.[6,35,36] The fact that the SCR activity does not depend on the Brønsted acid can be reconciled by realizing that there are usually more Brønsted acid sites than Lewis acid sites in zeolites;

only a small portion of Brønsted acid sites would take part in the SCR while Lewis acid sites are saturated with the reaction. Therefore, the amount of Brønsted acid sites would not significantly influence the SCR activity.

The pathway of NO oxidation we presented in this contribution is also different from the literature works. Janssens *et al.*[11] suggested that NO and O_2 would react on the Cu^+ site to form $Cu^{2+}NO_3^-$, followed by the oxidation with another NO to produce NO_2 and $Cu^{2+}NO_2^-$. Our mechanism, on the other hand, do not include NO_3^- species in the NO oxidation since our DFT calculations showed that the free energy of $Cu^{2+}NO_3^-$ is rather high. However, both Janssens *et al.* and we agree that NO oxidation is the rate-limiting step, and all the elementary steps involved in the fast SCR are also parts of the standard SCR. It seems contradictory to the work of Tronconi *et al.*,[50,75] who observed that the rate of NO oxidation is much slower than SCR process. This puzzle can be understood from Fig. 7. We can see that the NO oxidation in SCR is part of the reaction cycle rather than a isolated step; the NO oxidation alone would be slow in zeolite since most Cu site in zeolites are Cu^{2+} without the SCR redox cycle, while NO oxidation is favoured only when the site is reduced to Cu^+.[11]

General discussion of the zeolite chemistry

In the last several decades, zeolites have been widely used in the fields of petrochemical industry, fine chemicals, and other heterogeneous reactions.[79–82] As crystalline microporous materials, zeolites own many novel properties, such as species migration, ion exchange, and adsorption, which give us more efficient and cheap alternatives for some traditional catalytic reactions. The relation between the structure of Cu-SAPO-34 zeolites and activities of SCR process, however, has not been well understood. We therefore make a general discussion about its structure-activity relationship in this subsection, aiming to supplement current understandings on zeolite chemistry in general.

Starting from an isolated Cu^{2+} ion, the first step of SCR is the N–N coupling between

NO and NH_3 that goes through a small barrier (0.28 eV). One question naturally arises here: why can NO be activated with such a low energy barrier? The origin lies in the special zeolite structure: in Cu-SAPO-34, the diameter of the six-membered ring is about $5 \sim 6$ Å, and the structure of transition state (Fig. 3) fits such a ring well for the N–N coupling; the whole molecule (NH_2NO) bridges from the Cu ion to a O in the framework with a quite reasonable structure. One of H in the NH_3 will interact with this O by the hydrogen bond, thus lowering the energy of the transition state. Meanwhile, the six-membered ring will also stretch to some extent to fit the structure of transition states owing to the flexibility of zeolite framework. Moreover, the weakened N–H bond of the transition state also provides its N more space to couple with another N. These features of zeolites may partly explain their good performance on NH_3-SCR. Therefore, it was reasonable that the N–N coupling process over Cu-SSZ-13 goes through a similar pathway since the geometrical structures of SAPO-34 and SSZ-13 are similar.

Equally important, deep insight into the redox cycle in zeolites has been achieved in this work. From Fig. 7, we can notice that the valence of Cu ion in Cu$-NH_2NO$/H, Cu/H, and Cu/NH_4 are +1 while for the rest species it is +2 (measured by the Bader charge analysis, details in Tab. S3). The redox cycle is very important in the whole SCR process especially for the standard SCR, since Cu^{2+} is not able to activate O_2 molecules and the involvement of Cu^+ is crucial for NO oxidation according to the results in the last section. Aiming to clarify the role of zeolites in such a redox cycle, we calculated the valence number of each atom in the six-membered ring of Cu^{2+} and Cu^+ (Fig. 8ab). In Fig. 8b, one H remains on the O in the framework after the N–N coupling, and most of its electron will transfer to the Cu through the framework, which eventually reduces Cu^{2+} into Cu^+. Moreover, isosurfaces of charge density difference before and after O_2 adsorption on these two Cu sites are presented in Fig. 8cd. It is clear from Fig. 8c that the bonding between O_2 molecule and Cu^{2+} is very limited, because it is difficult for Cu^{2+} to donate electrons to O_2, because it is on the highest oxidation state. On the other hand, we can see from Fig. 8d that ceCu+ has a considerable

interaction with O_2 by electron accumulation on O_2 and depletion on Cu^+. According to the Bader charge analysis, the valence of Cu and two O atoms before and after adsorption are 0.69, 0, 0, and 1.01, -0.25, -0.1, respectively, indicating that 0.35 electrons are donated from Cu ion and the framework to O_2, and Cu^+ partly resumes to Cu^{2+}. Therefore, the O–O bond in the O_2 molecule is activated upon adsorption on Cu^+, leading to a stronger O_2 adsorption energy and lower energy barrier for NO oxidation.

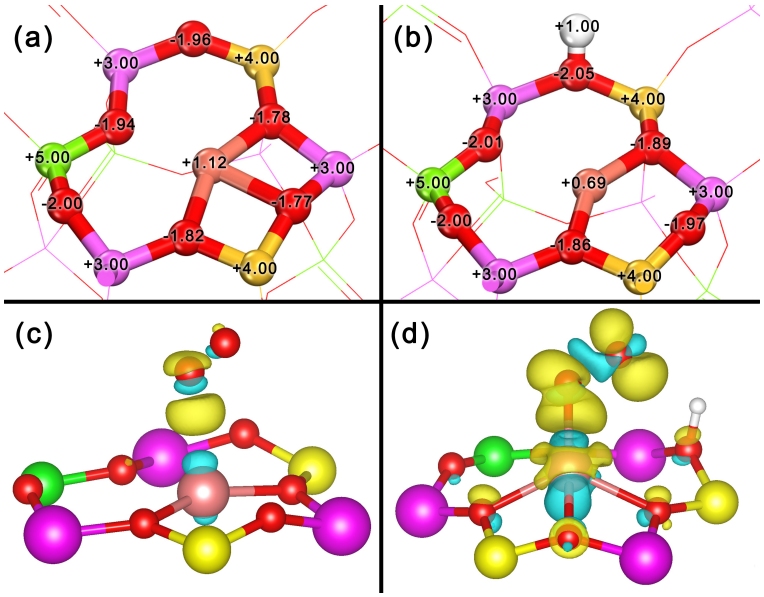

Figure 8: Bader charge of the six-membered ring loaded with Cu^{2+}(a) and Cu^+(b); isosurfaces (level: 0.0025) of charge density difference before and after O_2 adsorption on Cu^{2+}(c) and Cu^+(d). Yellow indicates the electronic accumulation and light blue for depletion.

In addition to the Lewis acid site (Cu ion), the last part of SCR process, the decomposition of NH_2NO, occurs on the Brønsted acid site with moderate energy barriers. Our calculations show that the adsorption free energy of NH_2NO on the Cu site is close to zero; therefore, it could readily transfer to Brønsted acid sites in the cage. NH_2NO is difficult to decompose on the Lewis acid sites due to a large intra-molecular proton transfer barrier, while the Brønsted acid sites can facilitate this process by a hydrogen push-pull mechanism. It means that Brønsted acid and Lewis acid sites collectively catalyse the reaction, and such a "multi-site" concept of catalysis is receiving increasingly attention in recent years.[64,83]

Finally, both similarities and differences can be found comparing the SCR activity on

traditional metal oxide catalysts with zeolites. In metal oxides (*e.g.* MnO_2 and V_2O_5), it is possible for NH_3 to donate one H to surface O with a reasonable barrier,[84,85] but such a pathway is not practical on zeolites since the ability of zeolite framework to accept H is inferior to that of oxides. On CHA-type zeolites, the six-membered ring serves as a bridge to facilitate the coupling of N–N bond as well as the breaking of N–H bond in NH_3. On the other hand, there is a similar concept of redox cycle of active site and interplay between the Brønsted acid and Lewis acid sites on traditional catalysts. Taking V_2O_5 as an example, V^{5+}, which serves as Lewis acid site, will be reduced to V^{4+} when NO react NH_3 to produce N_2 and H_2O; it then resumes to V^{5+} during NO oxidation. The Brønsted acid site (H) over metal oxides can also facilitate NH_2NO decomposition process.

Conclusion

In this work, a comprehensive investigation of NH_3-SCR process over Cu-SAPO-34 zeolites was carried out by virtue of periodic DFT calculations using hybrid functional. Van der Waals (vdW) interactions were also considered throughout the calculation, the main conclusions of which are the following:

(i) A detailed step-by-step NH_3-SCR mechanism over Cu-SAPO-34 was obtained with moderate energy barriers and reasonable intermediate structures.

(ii) A NO-assisted N–H bond breaking mechanism of NH_3 was determined to account for the N–N formation between NO and NH_3. The NO is activated by binding with N in NH_3 to form NH_2NO while one of its N–H bond is weakened. The extra H would remain at the six-membered ring of the zeolite, reducing the original Cu^{2+} into Cu^{+}.

(iii) The NO oxidation by O_2 was shown to occur on reduced Cu site (Cu^{+}), and the Cu^{+} will resume to Cu^{2+} after oxidation, completing the Cu^{2+}/Cu^{+} redox cycle.

(iv) A detailed decomposition mechanism of NH_2NO in the Brønsted acid site was iden-

tified, confirming not only its feasibility, but also a collective efforts of Brønsted acid and Lewis acid (Cu^{2+}) sites in catalysing NH_3-SCR over Cu-SAPO-34 zeolites.

The relation of above conclusions to the structural and electronic properties of zeolites, including their special six-membered ring structure, influence of the framework H on the valence of loaded metal ion, collective efforts by Brønsted acid and Lewis acid sites, are discussed and compared with previous literatures. These features may be extended to other catalytic reactions over zeolites and would supplement current understandings on not only SCR over Cu-CHA but also on general zeolite chemistry.

Acknowledgement

This project is supported by National Key Basic Research Program of China (2013CB933201), National Natural Science Foundation of China (21303052, 21333003, 21622305), Shanghai Rising-Star Program (14QA1401100), Chen Guang project (13CG24), Young Elite Scientist Sponsorship Program by CAST, Fundamental Research Funds for the Central Universities and Special Program for Applied Research on Super Computation of the NSFC-Guangdong Joint Fund (the second phase). The authors gratefully acknowledge UK's national high performance computing service ARCHER (for which access was obtained via the UKCP consortium) for computing time. Y.M. thanks the Queen's University of Belfast and Chinese Scholarship Council for a joint scholarship.

Supporting Information Available

Details of additional notes, structures, and energies mentioned in the paper.

This material is available free of charge via the Internet at `http://pubs.acs.org/`.

References

(1) Li, J. H.; Chang, H. Z.; Ma, L.; Hao, J. M.; Yang, R. T. *Catal. Today* **2011**, *175*, 147–156.

(2) Liu, F.; Yu, Y.; He, H. *Chem. Commun.* **2014**, *50*, 8445–8463.

(3) Mao, Y.; Wang, H.-F.; Hu, P. *Int. J. Quantum Chem.* **2015**, *115*, 618–630.

(4) Beale, A. M.; Gao, F.; Lezcano-Gonzalez, I.; Peden, C. H. F.; Szanyi, J. *Chem. Soc. Rev.* **2015**, *44*, 7371–7405.

(5) Koebel, M.; Elsener, M.; Kleemann, M. *Catal. Today* **2000**, *59*, 335–345.

(6) Li, J.; Li, S. H. *J. Phys. Chem. C* **2008**, *112*, 16938–16944.

(7) Bauerle, G. L.; Wu, S. C.; Nobe, K. *Ind. Eng. Chem. Prod. R & D* **1978**, *17*, 117–122.

(8) Liu, Z.; Zhang, S.; Li, J.; Zhu, J.; Ma, L. *Appl. Catal. B-Environ.* **2014**, *158-159*, 11–19.

(9) Beale, A. M.; Lezcano-Gonzalez, I.; Maunula, T.; Palgrave, R. G. *Catal. Struct. React.* **2014**, *1*, 25–34.

(10) Brandenberger, S.; Krocher, O.; Tissler, A.; Althoff, R. *Catal. Rev. Sci. Eng.* **2008**, *50*, 492–531.

(11) Janssens, T. V. W.; Falsig, H.; Lundegaard, L. F.; VennestrÃÿm, P. N. R.; Rasmussen, S. B.; Moses, P.; Giordanino, F.; Borfecchia, E.; Lomachenko, K. A.; Lamberti, C. et al. *ACS Catal.* **2015**, *5*, 2832–2845.

(12) Paolucci, C.; Parekh, A. A.; Khurana, I.; Di Iorio, J. R.; Li, H.; Albarracin Caballero, J. D.; Shih, A. J.; Anggara, T.; Delgass, W. N.; Miller, J. T. et al. *J. Am. Chem. Soc.* **2016**, *138*, 6028–6048.

(13) Nova, I.; Tronconi, E. *Urea-SCR Technology for deNOx After Treatment of Diesel Exhausts*; Springer-Verlag: New York, 2014.

(14) Kwak, J. H.; Tonkyn, R. G.; Kim, D. H.; Szanyi, J.; Peden, C. H. F. *J. Catal.* **2010**, *275*, 187–190.

(15) Ma, L.; Cheng, Y. S.; Cavataio, G.; McCabe, R. W.; Fu, L. X.; Li, J. H. *Appl. Catal. B-Environ.* **2014**, *156*, 428–437.

(16) Lezcano-Gonzalez, I.; Wragg, D. S.; Slawinski, W. A.; Hemelsoet, K.; Deyne, A.; Waroquier, M.; Speybroeck, V.; Beale, A. M. *J. Phys. Chem. C* **2015**, *119*, 24393–24403.

(17) Gao, F.; Washton, N. M.; Wang, Y.; KollÃąr, M.; Szanyi, J.; Peden, C. H. F. *J. Catal.* **2015**, *331*, 25–38.

(18) Andersen, C. W.; Bremholm, M.; Vennestrom, P. N. R.; Blichfeld, A. B.; Lundegaard, L. F.; Iversen, B. B. *IUCrJ* **2014**, *1*, 382–386.

(19) Deka, U.; Lezcano-Gonzalez, I.; Warrender, S. J.; Picone, A. L.; Wright, P. A.; Weckhuysen, B. M.; Beale, A. M. *Micropor. Mesopor. Mat.* **2013**, *166*, 144–152.

(20) Gao, F.; Walter, E. D.; Karp, E. M.; Luo, J.; Tonkyn, R. G.; Kwak, J. H.; Szanyi, J.; Peden, C. H. F. *J. Catal.* **2013**, *300*, 20–29.

(21) Wang, D.; Zhang, L.; Li, J. H.; Kamasamudram, K.; Epling, W. S. *Catal. Today* **2014**, *231*, 64–74.

(22) Yu, T.; Wang, J.; Shen, M. Q.; Li, W. *Catal. Sci. Technol.* **2013**, *3*, 3234–3241.

(23) McEwen, J. S.; Anggara, T.; Schneider, W. F.; Kispersky, V. F.; Miller, J. T.; Delgass, W. N.; Ribeiro, F. H. *Catal. Today* **2012**, *184*, 129–144.

(24) Goltl, F.; Bulo, R. E.; Hafner, J.; Sautet, P. *J. Phys. Chem. Lett.* **2013**, *4*, 2244–2249.

(25) Bates, S. A.; Verma, A. A.; Paolucci, C.; Parekh, A. A.; Anggara, T.; Yezerets, A.; Schneider, W. F.; Miller, J. T.; Delgass, W. N.; Ribeiro, F. H. *J. Catal.* **2014**, *312*, 87–97.

(26) Borfecchia, E.; Lomachenko, K. A.; Giordanino, F.; Falsig, H.; Beato, P.; Soldatov, A. V.; Bordiga, S.; Lamberti, C. *Chem. Sci.* **2015**, *6*, 548–563.

(27) Goltl, F.; Sautet, P.; Hermans, I. *Catal. Today* **2016**, *267*, 41–46.

(28) Paolucci, C.; Verma, A. A.; Bates, S. A.; Kispersky, V. F.; Miller, J. T.; Gounder, R.; Delgass, W. N.; Ribeiro, F. H.; Schneider, W. F. *Angew. Chem. Int. Ed.* **2014**, *53*, 11828–33.

(29) Korhonen, S. T.; Fickel, D. W.; Lobo, R. F.; Weckhuysen, B. M.; Beale, A. M. *Chem. Commun.* **2011**, *47*, 800–802.

(30) Beale, A. M.; Lezcano-Gonzalez, I.; Slawinksi, W. A.; Wragg, D. S. *Chem. Comm.* **2016**, *52*, 6170–6173.

(31) Fickel, D. W.; Lobo, R. F. *J. Phys. Chem. C* **2010**, *114*, 1633–1640.

(32) Deka, U.; Juhin, A.; Eilertsen, E. A.; Emerich, H.; Green, M. A.; Korhonen, S. T.; Weckhuysen, B. M.; Beale, A. M. *J. Phys. Chem. C* **2012**, *116*, 4809–4818.

(33) Gao, F.; Walter, E. D.; Kollar, M.; Wang, Y.; Szanyi, J.; Peden, C. H. F. *J. Catal.* **2014**, *319*, 1–14.

(34) Xue, J.; Wang, X.; Qi, G.; Wang, J.; Shen, M.; Li, W. *J. Catal.* **2013**, *297*, 56–64.

(35) Bruggemann, T. C.; Keil, F. J. *J. Phys. Chem. C* **2008**, *112*, 17378–17387.

(36) Li, J.; Li, S. *Phys. Chem. Chem. Phys.* **2007**, *9*, 3304–11.

(37) Bates, S. A.; Delgass, W. N.; Ribeiro, F. H.; Miller, J. T.; Gounder, R. *J. Catal.* **2014**, *312*, 26–36.

(38) Szanyi, J.; Kwak, J. H.; Zhu, H.; Peden, C. H. F. *Phys. Chem. Chem. Phys.* **2013**, *15*, 2368–2380.

(39) Giordanino, F.; Borfecchia, E.; Lomachenko, K. A.; Lazzarini, A.; Agostini, G.; Gallo, E.; Soldatov, A. V.; Beato, P.; Bordiga, S.; Lamberti, C. *J. Phys. Chem. Lett.* **2014**, *5*, 1552–1559.

(40) Uzunova, E. L.; Mikosch, H.; St. Nikolov, G. *Int. J. Quantum Chem.* **2013**, *113*, 723–728.

(41) Fulton, J. L.; Hoffmann, M. M.; Darab, J. G.; Palmer, B. J.; Stern, E. A. *J. Phys. Chem. A* **2000**, *104*, 11651–11663.

(42) Kwak, J. H.; Varga, T.; Peden, C. H. F.; Gao, F.; Hanson, J. C.; Szanyi, J. *J. Catal.* **2014**, *314*, 83–93.

(43) Goltl, F.; Hafner, J. *J. Chem. Phys.* **2012**, *136*, 064501.

(44) Kispersky, V. F.; Kropf, A. J.; Ribeiro, F. H.; Miller, J. T. *Phys. Chem. Chem. Phys.* **2012**, *14*, 2229–2238.

(45) Gunter, T.; Carvalho, H. W. P.; Doronkin, D. E.; Sheppard, T.; Glatzel, P.; Atkins, A. J.; Rudolph, J.; Jacob, C. R.; Casapu, M.; Grunwaldt, J.-D. *Chem. Comm.* **2015**, *51*, 9227–9230.

(46) Gao, F.; Kwak, J. H.; Szanyi, J.; Peden, C. H. F. *Top. Catal.* **2013**, *56*, 1441–1459.

(47) Yu, T.; Hao, T.; Fan, D.; Wang, J.; Shen, M.; Li, W. *The Journal of Physical Chemistry C* **2014**, *118*, 6565–6575.

(48) Doronkin, D. E.; Casapu, M.; GÃijnter, T.; MÃijller, O.; Frahm, R.; Grunwaldt, J.-D. *The Journal of Physical Chemistry C* **2014**, *118*, 10204–10212.

(49) Chen, H.-Y.; Sun, Q.; Wen, B.; Yeom, Y.-H.; Weitz, E.; Sachtler, W. M. H. *Catal. Today* **2004**, *96*, 1–10.

(50) Ruggeri, M. P.; Nova, I.; Tronconi, E. *Top. Catal.* **2013**, *56*, 109–113.

(51) Bruggemann, T. C.; Keil, F. J. *J. Phys. Chem. C* **2011**, *115*, 23854–23870.

(52) Krukau, A. V.; Vydrov, O. A.; Izmaylov, A. F.; Scuseria, G. E. *The Journal of Chemical Physics* **2006**, *125*, 224106.

(53) Heyd, J.; Scuseria, G. E. *The Journal of Chemical Physics* **2004**, *121*, 1187–1192.

(54) Heyd, J.; Scuseria, G. E.; Ernzerhof, M. *The Journal of Chemical Physics* **2003**, *118*, 8207–8215.

(55) Kresse, G.; Furthmüller, J. *Comp. Mater. Sci.* **1996**, *6*, 15–50.

(56) Kresse, G.; Hafner, J. *Phys. Rev. B* **1994**, *49*, 14251–14269.

(57) Grimme, S.; Antony, J.; Ehrlich, S.; Krieg, H. *J. Chem. Phys.* **2010**, *132*, 154104.

(58) Blöchl, P. E.; Jepsen, O.; Andersen, O. K. *Phys. Rev. B* **1994**, *49*, 16223–16233.

(59) Kresse, G.; Joubert, D. *Phys. Rev. B* **1999**, *59*, 1758–1775.

(60) Liu, Z.-P.; Hu, P. *J. Am. Chem. Soc.* **2003**, *125*, 1958–1967.

(61) Alavi, A.; Hu, P.; Deutsch, T.; Silvestrelli, P. L.; Hutter, J. *Phys. Rev. Lett.* **1998**, *80*, 3650–3653.

(62) Perdew, J. P.; Burke, K.; Ernzerhof, M. *Phys. Rev. Lett.* **1996**, *77*, 3865–3868.

(63) Wang, Z.; Cao, X. M.; Zhu, J.; Hu, P. *J. Catal.* **2014**, *311*, 469–480.

(64) Wang, Z.; Wang, H.-F.; Hu, P. *Chem. Sci.* **2015**, *6*, 5703–5711.

(65) Lok, B. M.; Messina, C. A.; Patton, R. L.; Gajek, R. T.; Cannan, T. R.; Flanigen, E. M. *J. Am. Chem. Soc.* **1984**, *106*, 6092–6093.

(66) Petitto, C.; Delahay, G. *Chem. Eng. J.* **2015**, *264*, 404–410.

(67) Wang, J.; Yu, T.; Wang, X. Q.; Qi, G. S.; Xue, J. J.; Shen, M. Q.; Li, W. *Appl. Catal. B-Environ.* **2012**, *127*, 137–147.

(68) Uzunova, E. L.; Mikosch, H.; Hafner, J. *J. Phys. Chem. C* **2008**, *112*, 2632–2639.

(69) Smith, L.; Cheetham, A. K.; Morris, R. E.; Marchese, L.; Thomas, J. M.; Wright, P. A.; Chen, J. *Science* **1996**, *271*, 799–802.

(70) Termath, V.; Haase, F.; Sauer, J.; Hutter, J.; Parrinello, M. *J. Am. Chem. Soc.* **1998**, *120*, 8512–8516.

(71) Uzunova, E. L.; Goltl, F.; Kresse, G.; Hafner, J. *J. Phys. Chem. C* **2009**, *113*, 5274–5291.

(72) Uzunova, E. L.; Mikosch, H.; Hafner, J. *J. Mol. Struc.-Theochem* **2009**, *912*, 88–94.

(73) Smith, L.; Cheetham, A.; Marchese, L.; Thomas, J.; Wright, P.; Chen, J.; Gianotti, E. *Catal. Lett.* **1996**, *41*, 13–16.

(74) Shi, L.; Yu, T.; Wang, X. Q.; Wang, J.; Shen, M. Q. *Acta Phys-Chim. Sin.* **2013**, *29*, 1550–1557.

(75) Ruggeri, M. P.; Selleri, T.; Colombo, M.; Nova, I.; Tronconi, E. *J. Catal.* **2014**, *311*, 266–270.

(76) Verma, A. A.; Bates, S. A.; Anggara, T.; Paolucci, C.; Parekh, A. A.; Kamasamudram, K.; Yezerets, A.; Miller, J. T.; Delgass, W. N.; Schneider, W. F. et al. *J. Catal.* **2014**, *312*, 179–190.

(77) Anstrom, M.; Topsøe, N.-Y.; Dumesic, J. A. *J. Catal.* **2003**, *213*, 115–125.

(78) Cheng, J.; Hu, P.; Ellis, P.; French, S.; Kelly, G.; Lok, C. M. *J. Phys. Chem. C* **2008**, *112*, 1308–1311.

(79) Weckhuysen, B. M.; Yu, J. *Chem. Soc. Rev.* **2015**, *44*, 7022–7024.

(80) Li, Y.; Yu, J. *Chem. Rev.* **2014**, *114*, 7268–7316.

(81) Van Speybroeck, V.; Hemelsoet, K.; Joos, L.; Waroquier, M.; Bell, R. G.; Catlow, C. R. A. *Chem. Soc. Rev.* **2015**, *44*, 7044–7111.

(82) Peng, C.; Wang, H. F.; Hu, P. *Phys. Chem. Chem. Phys.* **2016**, *18*, 14495–14502.

(83) Burch, R.; Paun, C.; Cao, X. M.; Crawford, P.; Goodrich, P.; Hardacre, C.; Hu, P.; McLaughlin, L.; Sa, J.; Thompson, J. M. *J. Catal.* **2011**, *283*, 89–97.

(84) Janssen, F. J. J. G.; Van den Kerkhof, F. M. G.; Bosch, H.; Ross, J. R. H. *J. Phys. Chem.* **1987**, *91*, 6633–6638.

(85) Soyer, S.; Uzun, A.; Senkan, S.; Onal, I. *Catal. Today* **2006**, *118*, 268–278.

Graphical TOC Entry

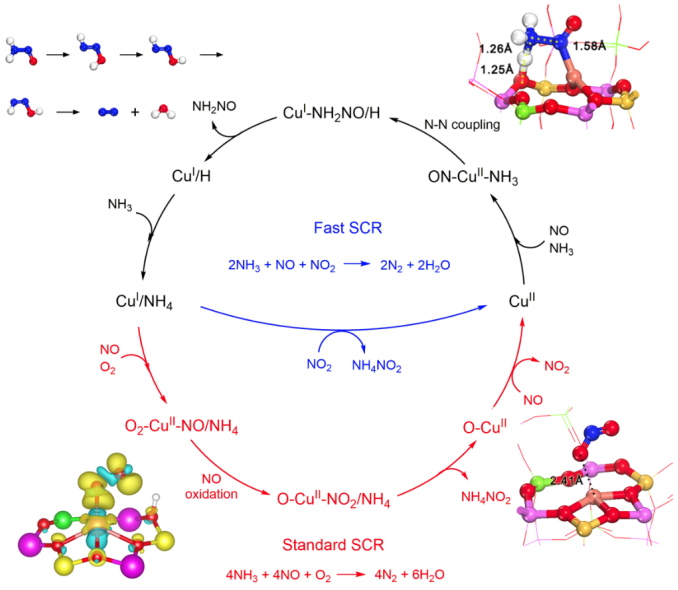

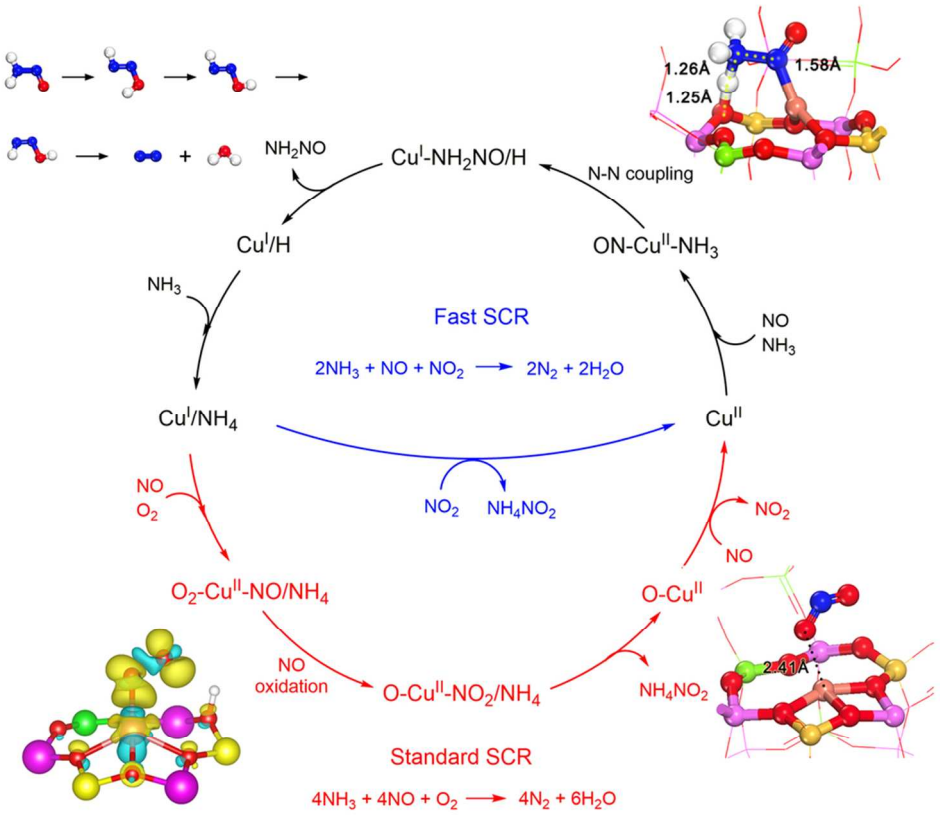

45x38mm (600 x 600 DPI)